Article citation info:
Devakaran KP, Arunshankar J. Engine NO_x control of SCR system using sliding mode controller. Combustion Engines. 0000;XXX(X):xx-xx. https://doi.org/10.19206/CE-225504

Karaiellapalayam Palanisamy DEVAKARAN
Jayabalan ARUNSHANKAR

Combustion Engines
Polish Scientific Society of Combustion Engines

Engine NO_x control of the SCR system using a sliding mode controller

ARTICLE INFO

Received: 13 March 2026
Revised: 20 May 2026
Accepted: 6 July 2026
Available online: 17 August 2026

The selective catalytic reduction system (SCR) uses aqueous NH_3 and a catalyst for reducing the NO_x emission emitted by the compression ignition (CI) engine exhaust. Due to stringent emission regulations and the growing demand for SCR systems, significant improvements in urea injection strategies and catalyst activity are required to reduce exhaust gas by-products. In this study, an SCR system combined with a super-twisting sliding mode controller (STSMC) is employed to regulate the exhaust gases of CI engines. The SCR system is represented by linearized state-space models of third and fourth order. The US06 emission cycle is used to determine the engine exhaust NO_x characteristics, which are then fed into the SCR system. According to the simulation results, the fourth order SCR model has a better de-NO_x conversion rate and less NH_3 slip than the third order SCR model, due to the fast-SCR kinematics.

Key words: *CI engine, NO_x, SCR, super-twisting sliding mode controller, US06*

1. Introduction

IC engines remain the most popular for automotive applications [8, 21]. The primary pollutant emitted from the exhaust of CI engines is NO_x, and its stringent emission norms have become increasingly stringent in recent decades [7, 18]. The urea-based SCR system has great potential and widespread acceptance for reducing NO_x emission [4, 13]. The SCR system uses aqueous NH_3, which reacts with exhaust NO_x in the presence of a catalyst to convert them into N_2 and H_2O, reducing tailpipe emissions [10]. Controlling exhaust NO_x and NH_3 slip under engine operating conditions with an effective catalyst remains a major challenge for the SCR system in real time [26]. Excessive NH_3 dosing causes ammonia slip, and inadequate NH_3 dosing causes NO_x slip by the SCR system [25].

A dual-cell SCR system for a diesel engine is designed, and a fuzzy logic controller is used for urea dosing to enhance NO_x conversion efficiency and reduce NH_3 tailpipe emissions [27]. A three state SCR model is developed and SMC is designed to control the NO_x and NH_3 pollutants [3]. A singular perturbation approach is used to separate tailpipe NO_x from NH_3 and to predict the NH_3 coverage factor of the urea-SCR system using the NO_x sensor [15]. An SMC is considered a reliable controller for advanced nonlinear systems, subjected to parametric uncertainties and external perturbations [1, 17]. The primary aspect of SMC is that it modifies the system dynamics by selecting a suitable switching function, keeping its closed-loop response unaffected by system uncertainties [5]. Super Twisting is one of the higher order SMC that minimizes the chattering effect without using the time derivatives of the sliding variable. [16].

Numerous investigations into SCR systems for IC engines have been carried out. However, stringent emission regulations have necessitated an advanced SCR system controller in order to reduce exhaust emissions. This study presents the use of DSTSMC in the SCR system to control NO_x emissions from the CI engine. The paper is organized as follows. NO_x emissions from the CI engine are discussed in Section 2. The methodology of the SCR system is briefed in Section 3. Sections 4 and 5 discuss the state space models of the SCR system. The controller design is briefed in Section 6. Section 7 discusses the results. Section 8 presents conclusions.

2. Exhaust NO_x emission for CI engine

This work follows the procedure published in [3] and [20]. The test bench consists of a medium-duty CI engine connected to a dynamometer. The test bench is started, and then the dynamometer load is applied to the engine. The diesel engine is tested over a sequence of US06 emission cycles, and the NO_x emissions are obtained [9] and [15]. The engine performance characteristics during the US06 cycle are listed in Table 1.

Table 1. CI engine performance characteristics

Time [s]	Engine speed [rpm]	Engine torque [Nm]	Exhaust gas flow rate [m³/s]	Exhaust gas temp [K]
0	1000	50	0.68	485
50	1200	100	0.05	508
100	2500	150	0.35	523
150	3000	200	0.05	548
200	2000	100	0.15	563
250	3500	250	0.05	588
300	4000	300	0.15	600
350	4500	280	0.05	623
400	3000	150	0.15	635
450	2000	100	0.05	645
500	1500	80	0.15	660
550	1000	60	0.05	675
600	800	40	0.15	685

As engine load increases, its combustion temperature rises, resulting in higher concentrations of C_{NO}, C_{NO2} emissions. Engine NO_x during US06 emission cycle is displayed in Fig. 1. The engine exhaust emission of C_{NO} is only considered for third order model, whereas the engine exhaust emission of both C_{NO} and C_{NO2} are considered for fourth order model [3]. The average $C_{NO,in}$ is 212 ppm for third-order model for US06 cycle. The average $C_{NO,in}$ and $C_{NO2,in}$ are 212 ppm and 60 ppm, for fourth order model for US06 cycle.

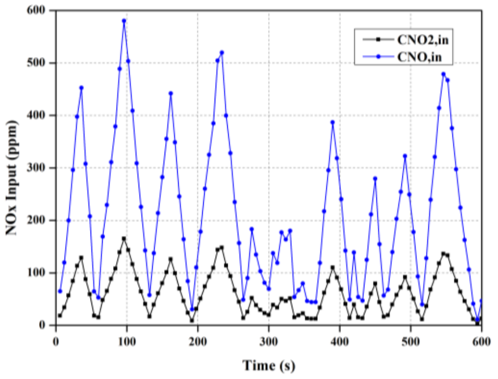

Fig. 1. Engine NO_x using US06

3. Methodology of the SCR system

The connection between the CI engine and the SCR system is shown in Fig. 2. A dynamometer is connected to a medium-duty V-8 automotive diesel engine at the inlet and the engine outlet is connected to the emission control system, which has a diesel oxidation catalyst (DOC), a diesel particulate filter (DPF) and a dual SCR catalyst [9, 11]. NO_x, NH_3, and thermocouple sensors are used to monitor the system. The SCR system injects aqueous NH_3 at the inlet. The dosing control unit determines the NH_3 injection quantity according to the sensors input [14]. A dual cell SCR is assumed to be a lumped single-cell SCR in this study.

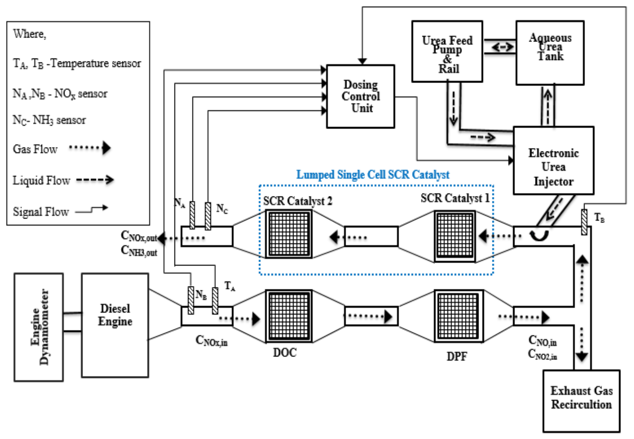

Fig. 2. Exhaust gas aftertreatment method using SCR

4. Third order model

4.1. Nonlinear model

The SCR model [24] and [14] is given by:

$$\begin{bmatrix}\dot{C}_{NO}\\ \dot{\theta}_{NH_3}\\ \dot{C}_{NH_3}\end{bmatrix}=\begin{bmatrix}-(r_{red}\emptyset_1\theta_{NH_3}C_{O_2}V+\frac{F}{V})\\ \frac{1}{\theta_{NH_3}}(r_{ads}C_{NH_3}V)-r_{ads}C_{NH_3}V-(r_{des}+r_{red}\,C_{NO}C_{O_2}V^2)\\ -\left[\emptyset_1 r_{ads}(1-\theta_{NH_3})+\frac{F}{V}\right]+\frac{1}{C_{NH_3}*V}(r_{des}\emptyset_1\theta_{NH_3})\end{bmatrix}\begin{bmatrix}C_{NO}\\ \theta_{NH_3}\\ C_{NH_3}\end{bmatrix}+\begin{bmatrix}0\\0\\ \frac{F}{V}\end{bmatrix}C_{NH_3,in}+\begin{bmatrix}\frac{F}{V}\\0\\0\end{bmatrix}C_{NO,in} \quad (1)$$

$$y=[1\quad 0\quad 0]\begin{bmatrix}C_{NO}\\ \theta_{NH_3}\\ C_{NH_3}\end{bmatrix} \quad (2)$$

The rate of SCR system (r_z)is modelled using the Arrhenius equation, which is given by:

$$r_z=K_z\exp\left[\frac{E_z}{RT}\right],\ \text{where } z\in\{r_{red}\,,r_{ads},\,r_{des}\} \quad (3)$$

where: r_{ads}, r_{des}, r_{red} are NH_3 adsorption, NH_3 desorption, and SCR reduction reaction rates, respectively. K_z is frequency constant and E_z is activation energy constant. V is the catalyst volume, T is the exhaust gas temperature, F is the exhaust flow rate, $\emptyset_1$ is ammonia storage capacity. C_{NH_3}, $C_{NH_3,in}$ are the concentration of ammonia at outlet and inlet, respectively. $C_{NO,in}$ and C_{NO} is the concentration of nitric oxide at inlet and outlet, respectively. C_{O_2} refers the oxygen concentration, θ_{NH_3} is the surface coverage fraction.

4.2 Linearized model

The nonlinear SCR model given in Eq. (1) and Eq. (2) are linearized [19, 24] as given in Table 2, and the resulting is:

$$\begin{bmatrix}\dot{C}_{NO}\\ \dot{\theta}_{NH_3}\\ \dot{C}_{NH3}\end{bmatrix}=\begin{bmatrix}A_{11}&A_{12}&0\\A_{21}&A_{22}&A_{23}\\0&A_{32}&A_{33}\end{bmatrix}\begin{bmatrix}C_{NO}\\ \theta_{NH_3}\\ C_{NH_3}\end{bmatrix}+\begin{bmatrix}0\\0\\ \frac{F}{V}\end{bmatrix}U+\begin{bmatrix}\frac{F}{V}\\0\\0\end{bmatrix}C_{NO,in} \quad (4)$$

$$y=[1\quad 0\quad 0]\begin{bmatrix}C_{NO}\\ \theta_{NH_3}\\ C_{NH_3}\end{bmatrix} \quad (5)$$

where:

$$A_{11}=-\emptyset_1 r_{red}\,C_{O_2}V\,\theta_{NH_3}-\frac{F}{V}$$

$$A_{12}=-\emptyset_1 r_{red}\,C_{O_2}V\,C_{NO}$$

$$A_{21}=-r_{red}\,C_{O_2}V^2\theta_{NH_3}$$

$$A_{22}=-r_{ads}\,V\,C_{NH_3}-(r_{des}+r_{red}\,C_{O_2}V^2\,C_{NO})$$

$$A_{23}=(1-\theta_{NH_3})r_{ads}V$$

$$A_{32}=(\emptyset_1 r_{ads}\,C_{NH_3})+\frac{(\emptyset\,r_{des})}{V}$$

$$A_{33}=-\left(-\emptyset_1 r_{ads}(1-\theta_{NH_3})+\frac{F}{V}\right)$$

Table 2. Engine exhaust characteristics

Operating Conditions	Values
Flow rate (F)	0.167 m^3/s
Temperature (T)	595 K
Oxygen concentration ($C_{O_2,in}$)	2 $moles/m^3$
Nitric oxide concentration ($C_{NO,in}$)	12 ppm
Nitrogen dioxide levels ($C_{NO_2,in}$)	4 ppm

Using the catalyst specifications and kinetic parameters [23] and [15] listed in Table 3 and Table 4 respectively, the result is:

$$\dot{X}(t)=A\,X(t)+B\,U(t)+E_1\,d_{CNO}(t) \quad (6)$$

$$Y(t)=H\,X(t) \quad (7)$$

where: $X(t)=\begin{bmatrix}X_1(t)\\X_2(t)\\X_3(t)\end{bmatrix}=\begin{bmatrix}C_{NO}\\\theta_{NH_3}\\C_{NH_3}\end{bmatrix}$, $U(t)$ is the input vector, $d_{CNO}(t)$ is NO inlet disturbance

$$A=\begin{bmatrix}-619.29 & -3.1\times10^{1} & 0\\ -5.48\times10^{-2} & -5.20\times10^{2} & 6.73\times10^{-2}\\ 0 & 5.72\times10^{6} & -7.57\times10^{2}\end{bmatrix} B=\begin{bmatrix}0\\0\\16.7\end{bmatrix} E_1=\begin{bmatrix}16.7\\0\\0\end{bmatrix}$$

Table 3. SCR catalyst specification

Specification	Values
Type	Cu-Zeolite
Volume (V)	0.005 m^3
Space velocity (F/V)	33 s^{-1}
C_{NH3} storage capacity ($\emptyset_1$)	120 moles/m^3
C_{NH3} desorption efficiency(δ_1, δ_2)	0.5 and 0.5
C_{NH3} coverage fraction (θ_{NH_3})	0.25

Table 4. SCR catalyst kinetic rate

Reaction	Frequency factor (K_z)	Activation energy (E_z)
Standard SCR (r_{red})	2.74×10^8 m^3/mol·s	76 kJ/mol
NH_3 adsorption (r_{ads})	6.8 m^3/mol·s	0 kJ/mol
NH_3 desorption (r_{des})	5.202×10^2 1/s	48 kJ/mol

4.3. Discrete model

The linear model given in Eq. (6) and Eq. (7) is discretized for 20 µs, the resulting is:

$$X(k+1)=A_d\,X(k)+B_d\,U(k)+E_{d_1}\,d_{CNO}(k) \quad (8)$$

$$Y(k)=H_d\,X(k) \quad (9)$$

where:

$$A_d=\begin{bmatrix}0.9877 & -0.0006 & -0.0000\\ -0.0000 & 0.9847 & 0.0000\\ -0.0001 & 112.9514 & 0.9850\end{bmatrix} B_d=\begin{bmatrix}0\\0\\3.31\times10^{-4}\end{bmatrix}$$

$$E_{d1}=\begin{bmatrix}3.18\times10^{-4}\\0\\0\end{bmatrix} H_d=[1 \quad 0 \quad 0]$$

5. Fourth order model

5.1. Nonlinear model

The SCR model [2] proposed by is given in Annex 1 – Eq. (10) and Eq. (11).

where $\emptyset$ is NH_3 storage capacity, with S_1 and S_2 as constants given by:

$$\emptyset=S_1\exp(S_2T) \quad (12)$$

The Arrhenius equations are used for the reaction rates(r_m), and given by:

$$r_m=K_m\exp\left[\frac{E_m}{RT}\right],\ \text{where } m\in\{r_a, r_b, r_c, r_{d1}, r_{d2}, r_e\} \quad (13)$$

$$r_a=K_1e^{-\left(\frac{E_1}{RT}\right)}C_{NO}\,C_{O_2}\theta_{NH_3}\emptyset\,V^2 \quad (14)$$

$$r_b=K_2e^{-\left(\frac{E_2}{RT}\right)}C_{NO}\,C_{NO_2}\theta_{NH_3}\emptyset\,V^2 \quad (15)$$

$$r_c=K_3e^{-\left(\frac{E_3}{RT}\right)}\,C_{O_2}\theta_{NH_3}\emptyset\,V\,\delta_1 \quad (16)$$

$$r_{d1}=K_{4F}e^{-\left(\frac{E_{4F}}{RT}\right)}\,C_{NH_3}(1-\theta_{NH_3})\emptyset\,V \quad (17)$$

$$r_{d2}=K_{4R}e^{-\left(\frac{E_{4R}}{RT}\right)}\theta_{NH_3}\emptyset\,\delta_2 \quad (18)$$

$$r_e=K_5e^{-\left(\frac{E_5}{RT}\right)}C_{NO}\,C_{O_2}V^2 \quad (19)$$

where: E_m is activation energy constant, K_m is frequency factor. The representation of reaction rates r_a is SCR, r_b is fast SCR, r_c is NH_3 oxidation, r_{d1} is ammonia adsorption, r_{d2} is ammonia desorption and r_e is NO oxidation, C_{NO_2} is outlet concentration of NO_2. δ_1 , δ_2 are NH_3 absorption and desorption efficiency, respectively. $C_{NO_2,in}$ is inlet concentration of NO_2, C_{NO} is the outlet concentration of NO and θ_{NH_3} is the surface coverage fraction.

5.2. Linearized model

The nonlinear SCR model given in Eq. (10) and Eq. (11) are linearized [2] and [19] given in Table 2, and resulting is:

$$\begin{bmatrix}\dot{C}_{NO}\\\dot{C}_{NO_2}\\\dot{\theta}_{NH_3}\\\dot{C}_{NH_3}\end{bmatrix}=\begin{bmatrix}A_{11} & A_{12} & A_{13} & 0\\ A_{21} & A_{22} & A_{23} & 0\\ A_{31} & A_{32} & A_{33} & A_{34}\\ 0 & 0 & A_{43} & A_{44}\end{bmatrix}\begin{bmatrix}C_{NO}\\C_{NO_2}\\\theta_{NH_3}\\C_{NH_3}\end{bmatrix}+\begin{bmatrix}0\\0\\0\\\frac{F}{V}\end{bmatrix}U+\begin{bmatrix}\frac{F}{V}\\0\\0\\0\end{bmatrix}C_{NO,in}+\begin{bmatrix}0\\\frac{F}{V}\\0\\0\end{bmatrix}C_{NO_2,in} \quad (20)$$

$$y=\begin{bmatrix}1 & 0 & 0 & 0\\ 0 & 1 & 0 & 0\end{bmatrix}\begin{bmatrix}C_{NO}\\C_{NO_2}\\\theta_{NH_3}\\C_{NH_3}\end{bmatrix} \quad (21)$$

where:

$$A_{11}=-r_a\,C_{O_2}\emptyset\,V\,\theta_{NH_3}-\frac{1}{2}r_b\emptyset\,V\,C_{NO_2}\theta_{NH_3}-r_e\,C_{O_2}V-\frac{F}{V}$$

$$A_{12}=-\frac{1}{2}r_b\emptyset\,V\,C_{NO}\,\theta_{NH_3}$$

$$A_{13}=-r_a\,C_{O_2}\emptyset\,VC_{NO}-\frac{1}{2}r_b\emptyset\,VC_{NO}\,C_{NO_2}$$

$$A_{21}=-\frac{1}{2}r_b\emptyset\,V\,C_{NO_2}\theta_{NH_3}+r_e\,C_{O_2}V$$

$$A_{22} = -\frac{1}{2} r_b \emptyset\, V C_{NO}\, \theta_{NH_3} - \frac{F}{V}$$

$$A_{23} = -\frac{1}{2} r_b \emptyset\, V C_{NO}\, C_{NO_2}$$

$$A_{31} = -(r_a\, C_{O_2} V^2 + r_b V^2 C_{NO_2})\theta_{NH_3}$$

$$A_{32} = -(r_b\, V^2 C_{NO})\theta_{NH_3}$$

$$A_{33} = -(r_{d1} V\, C_{NH_3} + r_c\, C_{O_2} V \delta_1 + r_{d2}\, \delta_2 + r_a\, C_{O_2} V^2 C_{NO} + r_b V^2 C_{NO}\, C_{NO_2})$$

$$A_{34} = -\theta_{NH_3}(r_{d1} V) + r_{d1} V$$

$$A_{43} = -\emptyset\, r_{d1}\, C_{NH_3} + \frac{1}{V}\, r_{d2} \emptyset\, \delta_2$$

$$A_{44} = -(\emptyset\, r_{d1}\, (1-\theta_{NH_3}) + \frac{F}{V})$$

Using the SCR catalyst specifications and, kinetic parameters [23] listed in Table 3 and Table 5 respectively, the result is:

$$\dot{X}(t) = A\, X(t) + B\, U(t) + E_1\, d_{CNO}(t) + E_2\, d_{CNO_2}(t) \tag{22}$$

$$Y(t) = H\, X(t) \tag{23}$$

where: $X(t) = \begin{bmatrix} X_1(t) \\ X_2(t) \\ X_3(t) \\ X_4(t) \end{bmatrix} = \begin{bmatrix} C_{NO} \\ C_{NO_2} \\ \theta_{NH_3} \\ C_{NH_3} \end{bmatrix}$,

$d_{CNO}(t)$ and $d_{CNO_2}(t)$ is NO and NO_2 inlet disturbances, respectively.

$$A = \begin{bmatrix} -42709.7 & -2.95\times10^4 & -2.22\times10^2 & 0 \\ -1.86\times10^4 & -2.95\times10^4 & -9.66\times10^1 & 0 \\ -5.57 & -5.36 & -7.35\times10^3 & -6.69\times10^{-2} \\ 0 & 0 & 67321.24916 & -129.12 \end{bmatrix}$$

$$B = \begin{bmatrix} 0 \\ 0 \\ 0 \\ 16.7 \end{bmatrix}$$

$$E_1 = \begin{bmatrix} 16.7 \\ 0 \\ 0 \\ 0 \end{bmatrix} \quad E_2 = \begin{bmatrix} 0 \\ 16.7 \\ 0 \\ 0 \end{bmatrix} \quad H = \begin{bmatrix} 1 & 0 & 0 & 0 \\ 0 & 1 & 0 & 0 \end{bmatrix}$$

Table 5. SCR catalyst kinetic rate

Reaction	Frequency factor (K_m)	Activation energy (E_m)
Standard SCR (r_a)	2.74×10^8 m^3/mol·s	75 kJ/mol
Fast SCR (r_b)	1.03×10^9 m^6/mol^2·s	40 kJ/mol
NH_3 oxidation (r_c)	1.02×10^5 1/s	87 kJ/mol
NH_3 Adsorption (r_{d1})	6.8 m^3/mol·s	0 kJ/mol
NH_3 Desorption (r_{d2})	5.2×10^2 1/s	47 kJ/mol
NO oxidation (r_e)	3.99×10^4 1/s	57 kJ/mol

5.3. Discrete model

The linear model given in Eq. (22) and Eq. (23) is discretized for 1 μs, the result is:

$$X(k+1) = A_d\, X(k) + B_d U(k) + E_{d1} d_{CNO}(k) + E_{d2}\, d_{CNO_2}(k) \tag{24}$$

$$Y(k) = H_d\, X(k) \tag{25}$$

where

$$A_d = \begin{bmatrix} 0.9585 & -0.0285 & -0.0002 & -0.0000 \\ -0.0179 & 0.9712 & -0.0001 & -0.0000 \\ -0.0000 & -0.0000 & 0.9927 & -0.0000 \\ -0.0000 & -0.0000 & 0.0671 & 0.9999 \end{bmatrix} B_d = \begin{bmatrix} 0.0000 \\ 0.0000 \\ -0.0000 \\ 1.67\times10^{-5} \end{bmatrix}$$

$$E_{d1} = \begin{bmatrix} 1.63\times10^{-5} \\ -0.0000 \\ -0.0000 \\ 0.0000 \end{bmatrix} E_{d2} = \begin{bmatrix} -0.0000 \\ 1.64\times10^{-5} \\ -0.0000 \\ -0.0000 \end{bmatrix} H = \begin{bmatrix} 1 & 0 & 0 & 0 \\ 0 & 1 & 0 & 0 \end{bmatrix}$$

6. Controller design

The first step is to identify a switching function [5], which results in

$$S = C^T X_d(k) \tag{26}$$

The switching function represents

$$S = C_1 X_1(k) + C_2 X_2(k) + \ldots + C_n X_n(k) = C^T X_d\,(k) = 0 \tag{27}$$

Quasi-sliding mode conditions [6] is given by

$$S(k+1) = S(k) = 0, \text{ where } k = 0,1,2,3,4\ldots \tag{28}$$

Sliding surface results in

$$C^T = [C_1 \quad C_2 \quad C_3 \;\; C_4 \cdots C_n]$$

where:

$$C_1 = (-1)^{n-1}\, (\lambda_1 \lambda_2 \ldots\ldots \lambda_{n-1}) \tag{29}$$

$$C_2 = (-1)^{n-2}\, (\lambda_2 \lambda_3 \ldots\ldots \lambda_{n-1} + \lambda_1 \lambda_3 \ldots . \lambda_{n-1} + \lambda_1 \lambda_2 \ldots . \lambda_{n-1})$$

$$C_{n-1} = (-1)\, (\lambda_1 + \lambda_2 + \lambda_3 + \ldots + \lambda_{n-1})$$

$$C_n = 1$$

with λ_1, $\lambda_2 \ldots \lambda_{n-1}$, are the desired eigen values. Choosing the appropriate eigenvalues yields the switching vector [6].

The second step is to find an appropriate controller that leads the system states to migrate on a switching surface. Super-Twisting Sliding Mode Controller (STSMC) is one of the best higher-order SMC [16] and [12], represented by:

$$U(k) = \lambda_{k1} |\, S(k)\, |^{\frac{1}{2}}\, \mathrm{sign}\big(S(k)\big) + U_1(k) \tag{30}$$

$$U_1(k+1) = U_1(k) + \lambda_{k2}\, \mathrm{sign}\,(S(k))$$

$$\mathrm{sign}\big(S(k)\big) = \begin{cases} 1, & S(k) > 0 \\ \in [-1,1], & S(k) = 0 \\ -1, & S(k) < 0 \end{cases} \tag{31}$$

where S(k) is the sliding variable. The tuning parameters of the controllers are denoted by λ_{k1} and λ_{k2}.

6.1. DSTSMC design for third order model

The open loop eigenvalues are $\lambda_{a1} = 0.9877$, $\lambda_{a2} = 0.999$, $\lambda_{a3} = 0.9749$. For the desired closed loop eigenvalues of $\lambda_{b1} = -0.3$, $\lambda_{b2} = -0.4$, the sliding surface resulting is:

$$C^T = [0.1200 \;\; 0.7000 \;\; 1.0000]$$

The controller tuning parameters resulted in $\lambda_{k1} = 17$ and $\lambda_{k2} = 4\times10^{-4}$.

6.2. DSTSMC design for fourth order model

The open loop eigen values are $\lambda_{c1} = 0.9413$, $\lambda_{c2} = 0.9883$, $\lambda_{c3} = 0.9927$, $\lambda_{c4} = 0.999$. For the desired closed loop eigenvalues of $\lambda_{d1} = -0.4$, $\lambda_{d2} = -0.3$, $\lambda_{d3} = -0.2$, the sliding surface resulting is

$$C^T = [0.0240 \quad 0.2600 \quad 0.9000 \quad 1.0000]$$

The tuning parameters of the controller resulted in $\lambda_{k1} = 0.3$ and $\lambda_{k2} = 1\times10^{-7}$.

7. Results and discussion

The performance of the SCR system with STSMC is simulated. The De-NO_x conversion efficiency, NH_3 reacted, and NH_3 slip of SCR system [22] are determined by:

$$\text{De-NO}_x \text{ efficiency} = 1 - \left(\frac{C_{NO,out}}{C_{NO,in}}\right) \quad (32)$$

$$NH_3 \ \text{Slip} = NH_3 \ \text{injected} - NH_3 \ \text{reacted} \quad (33)$$

$$NH_3 \ \text{reacted} = (C_{NO_x,in})\left(1 - \left(\frac{C_{NO,out}}{C_{NO,in}}\right)\right) \quad (34)$$

7.1. Outlet concentration of NO

The DSTSMC modifies the NH_3 injection in response to the inlet NO, and subsequently, the SCR system reacts to reduce NO emissions. From the results, third and fourth order SCR models have an average $C_{NO,out}$ of 4.9 ppm and 3.6 ppm, respectively, over 600 s. The outlet concentration of nitric oxide is shown in Fig. 3.

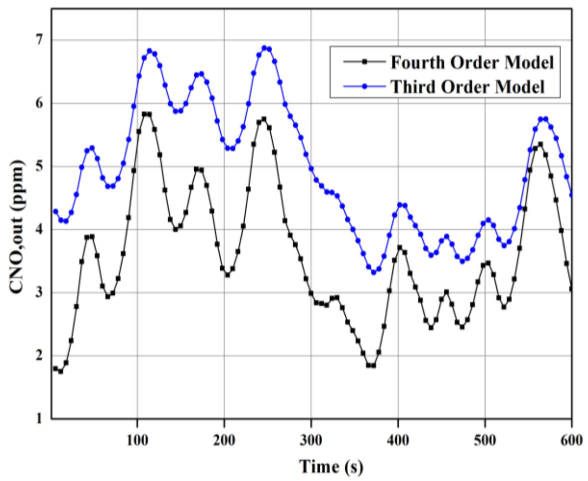

Fig. 3. Outlet concentration of nitric oxide

7.2. Outlet concentration of NO_2

The outlet concentration of Nitrogen di-oxide is displayed in Fig. 4. The SCR system reduces the average $C_{NO_{2,out}}$ to 1.4 ppm over 600 s for fourth order model.

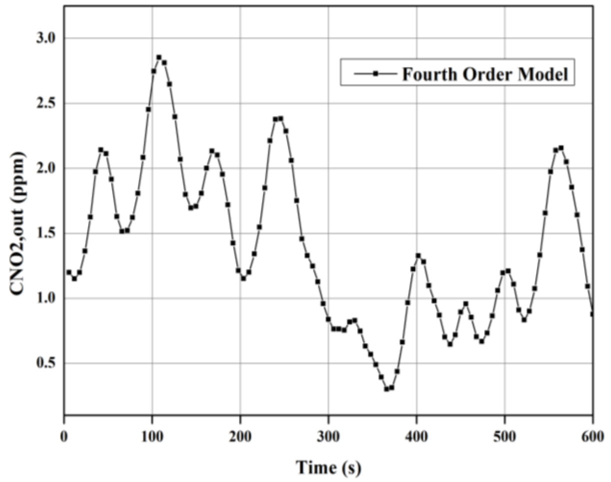

Fig. 4. Outlet concentration of nitrogen di-oxide

7.3. Ammonia reacted ratio

The SCR with STSMC maintains the C_{NH3} reacted ratio as 0.98:1 and 0.99:1 for third and fourth order models, respectively. The reacted ratio levels are equivalent to outlet concentration of oxides of nitrogen decreased by the SCR system. The ammonia reacted ratio is shown in Fig. 5. According to the results, the high catalytic activation rate of fast-SCR causes the fourth order model to react more quickly which produces less slip of exhaust gases.

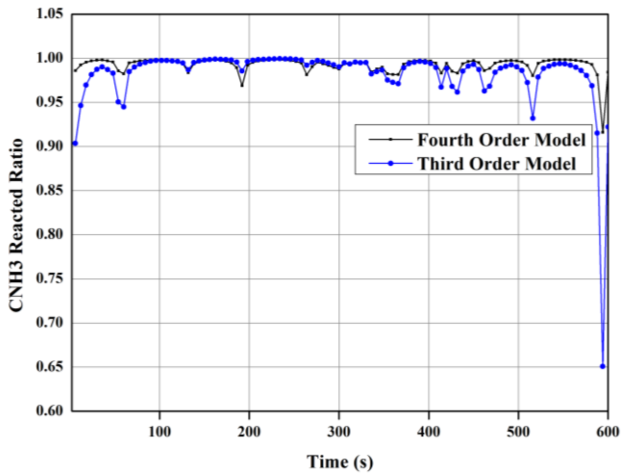

Fig. 5. Ammonia reacted ratio

7.4. De-NO_x efficiency

The C_{NO} conversion efficiencies are 95.7 % and 97% for the third and fourth order models, respectively. In addition, the fourth order model has C_{NO2} conversion efficiency of 96.2%. Therefore, the fourth order model has a total de-NO_x efficiency of 96.6%. Fig. 6 displays oxides of Nitrogen conversion efficiency. Hence, the SCR system meets the stringent emission standards.

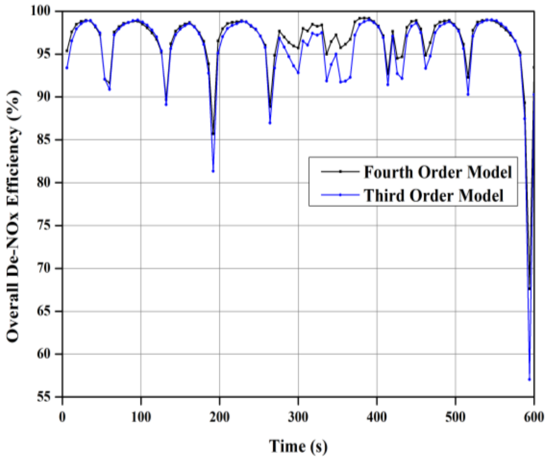

Fig. 6. Oxides of nitrogen conversion efficiency

7.5. Ammonia slip

The average C_{NH_3} slip of third and fourth order models are 1.77 ppm and 1.04 ppm, respectively over 600 s. The initial rise in NH_3 slip is caused by the controller overdosing, and the gain in de-NO_x conversion is negligible. The C_{NH_3} slip is presented in Fig. 7.

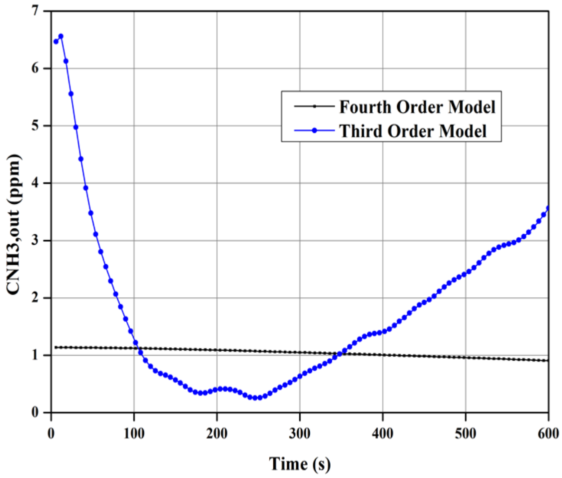

Fig. 7. Outlet concentration of ammonia

7.6. Ammonia injection ratio

The average C_{NH_3} injection ratio and the average usage of urea for third order model are 0.96:1 and 208 ppm, respectively, over 600 s. The average C_{NH_3} injection ratio and the average usage of urea for fourth order model are 0.97:1 and 268 ppm, respectively, over 600 s. The results show that the fourth order model utilizes more NH_3, but it exhibits a greater conversion rate with negligible NH_3 slip because to the fast-SCR kinetics. The ammonia injection ratio is shown in Fig. 8.

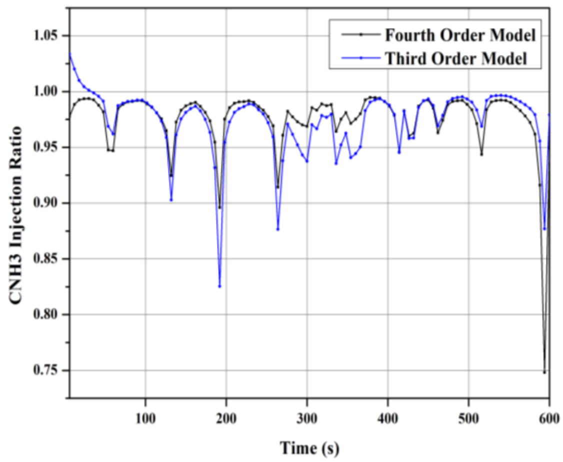

Fig. 8. Ammonia injection ratio

Conclusions

This work presents exhaust NO_x control for SCR system for automotive CI engine utilizing DSTSMC and the results are simulated. The third and fourth order SCR models exhibits de-NO_x conversion rate of 95.7% and 96.6%, respectively over 600 s. The average C_{NH3} slip for the third order model is 1.77 ppm over 600 seconds. The fourth order SCR model has an average C_{NH3} slip of 1.04 ppm over 600 seconds. The injection ratio and reacted ratio of ammonia to NO_x are enhanced for fourth order model due to fast-SCR kinetics. Hence, STSMC for the SCR system attains the targeted pollution norms for CI engines. In the future, an experimental validation of the SCR system in real-time using sensors and hardware for an automotive CI engine will be implemented. An on-board diagnostics-based SCR system with catalyst multi-functions such as catalyst ageing, thermal de-activation, and catalyst poising will be employed.

Nomenclature

BP	brake power
DOC	diesel oxidation catalyst
DPF	diesel particulate filter
IC	internal combustion
PM	particulate matter
SCR	selective catalytic reduction
SMC	sliding mode controller
STSMC	super-twisting sliding mode controller

Bibliography

[1] Ahmed SF, Raza Y, Mahdi HF, Muhamad WW, Joyo MK, Shah A et al. Review on sliding mode controller and its modified types for rehabilitation robots. 2019 IEEE 6th International Conference on Engineering Technologies and Applied Sciences (ICETAS) 2019 Dec 20, p. 1-8. https://doi.org/10.1109/ICETAS48360.2019.9117390

[2] Chen P, Wang J. Estimation and adaptive nonlinear model predictive control of selective catalytic reduction systems in automotive applications. J Process Contr. 2016;40:78-92. https://doi.org/10.1016/j.jprocont.2016.01.005

[3] Devarakonda M, Parker G, Johnson JH, Strots V, Santhanam S. Model-based estimation and control system development in

a urea-SCR aftertreatment system. SAE Int J Fuels and Lubr. 2009;1(1):646-661. https://doi.org/10.4271/2008-01-1324

[4] Dziubak T, Ślęzak M. Characteristics of pollutants emitted by motor vehicles and their impact on the environment and engine operation. Combustion Engines. 2025;200(1):37-55. https://doi.org/10.19206/CE-194628

[5] Gambhire SJ, Kishore DR, Londhe PS, Pawar SN. Review of sliding mode based control techniques for control system applications: Int J Dynam Control. 2021;9(1):363-378. https://doi.org/10.1007/s40435-020-00638-7

[6] Gao W, Wang Y, Homaifa A. Discrete-time variable structure control systems. IEEE Trans Ind Electron. 1995;42(2):117-122. https://doi.org/10.1109/41.370376

[7] Han J, Kim T, Jung H, Pyo S, Cho G, Oh Y et al. Improvement of NO_x reduction rate of urea SCR system applied for an non-road diesel engine. Int J Automot Technol. 2019;20(6):1153-1160. https://doi.org/10.1007/s12239-019-0108-6

[8] Hassan QH, Al-Abboodi H. Experimental investigation of the impact of methanol-diesel blends on diesel engine emissions and performance. Combustion Engines. 2025;201(2):150-157. https://doi.org/10.19206/CE-204494

[9] Hsieh MF, Wang J. Development and experimental studies of a control-oriented SCR model for a two-catalyst urea-SCR system. Control Eng Pract. 2011;19(4):409-422. https://doi.org/10.1016/j.conengprac.2011.01.004

[10] Devakaran KP, Jayabalan A. De-NOx conversion of selective catalytic reduction system for diesel engine using dual catalyst coated ceramic monoliths. Int J Chem React Eng. 2023;21(9):1141-1151. https://doi.org/10.1515/ijcre-2023-0027

[11] Ko A, Woo Y, Jang J, Jung Y, Pyo Y, Jo H et al. Complementary effects between NO oxidation of DPF and NO_2 decomposition of SCR in light-duty diesel engine. J Ind Eng Chem. 2019;80:160-170. https://doi.org/10.1016/j.jiec.2019.07.045

[12] Kuntanapreeda S. Super-twisting sliding-mode traction control of vehicles with tractive force observer. Control Eng Pract.2015;38:26-36. https://doi.org/10.1016/j.conengprac.2015.01.004

[13] Li Y, Liao J, Xu H, Wu Y, Cai Z, Hu J. Comprehensive experimental analysis of a diesel engine with an electrically heated catalyst and close-coupled SCR during cold/hot WHTC. Appl Therm Eng. 2025;262:125277. https://doi.org/10.1016/j.applthermaleng.2024.125277

[14] Lin Q, Chen P. A simple and effective methodology for estimating urea selective catalytic reduction systems states based on NO_x sensor measurement. 2017 American Control Conference (ACC) 2017 May 24 (p. 5367-5372). https://doi.org/10.23919/ACC.2017.7963789

[15] Lin Q, Chen P. Model-based analysis and control of SCR using NO_x sensor measurements. 2018 Annual American Control Conference (ACC) 2018 Jun 27 (p. 5522-5527). https://doi.org/10.23919/ACC.2018.8431141

[16] Liu J, Gao L, Zhang J, Yan F. Super-twisting algorithm second-order sliding mode control for collision avoidance system based on active front steering and direct yaw moment control. Proc Inst Mech Eng D: J Automob Eng. 2021;235(1):43-54. https://doi.org/10.1177/0954407020948298

[17] Ma Y, Wang J. Sliding-mode control of automotive selective catalytic reduction systems with state estimation. Proc Inst Mech Eng D: J Automob Eng. 2020;234(2-3):630-644. https://doi.org/10.1177/0954407019853968

[18] Mouzong FB, Bencherif M, Ayissi MZ. Performance and emissions of a diesel engine fueled by Tiska 68-based synthetic fuel blends. Combustion Engines. 2025;201(2):34-43. https://doi.org/10.19206/CE-202187

[19] Devakaran KP, Jayabalan A. Engine exhaust gas control of selective catalytic system using sliding mode controller. Emiss Control Sci Technol. 2024;10(2):244-254. https://doi.org/10.1007/s40825-024-00249-0

[20] Devakaran KP, Jayabalan A. Investigation of urea selective catalytic reduction system with catalyst coated ceramic monolith. J Ceram Process Res. 2021;22(1):79-85. https://doi.org/10.36410/jcpr.2021.22.1.79

[21] Rymaniak Ł, Pielecha J, Ziółkowski M, Sobczak J, Szymlet N. Comparison of pollutant emissions per passenger for public and individual transport. Combustion Engines. 2026;204(1):52-57. https://doi.org/10.19206/CE-210469

[22] Shen B, Li Z, Li J, Kong X, He L, Song J et al. Development of a 1D Urea-SCR system model coupling with wall film decomposition mechanism based on engine bench test data. Energy Procedia. 2017;142:3492-3497. https://doi.org/10.1016/j.egypro.2017.12.235

[23] Song X, Parker G, Johnson JH, Naber J, Pihl J. A modeling study of SCR reaction kinetics from reactor experiments. SAE Technical Paper. 2013-01-1576. 2013. https://doi.org/10.4271/2013-01-1576

[24] Upadhyay D, Van Nieuwstadt M. Model based analysis and control design of a urea-SCR deNO_x aftertreatment system. J Dyn Syst Meas Cont. 2006;128:737-741. https://doi.org/10.1115/1.2234494

[25] Vignesh R, Ashok B. Critical interpretative review on current outlook and prospects of selective catalytic reduction system for De-NOx strategy in compression ignition engine. Fuel. 2020;276:117996. https://doi.org/10.1016/j.fuel.2020.117996

[26] Xu HT, Luo ZQ, Wang N, Qu ZG, Chen J, An L. Experimental study of the selective catalytic reduction aftertreatment for the exhaust emission of a diesel engine. Appl Therma Eng. 2019;147:198-204. https://doi.org/10.1016/j.applthermaleng.2018.10.067

[27] You K, Wei L, Jiang K. A fuzzy logic urea dosage controller design for two-cell selective catalytic reduction systems. ISA Trans. 2018;78:21-30. https://doi.org/10.1016/j.isatra.2017.12.016

Karaiellapalayam Palanisamy Devakaran, DEng. – Department of Automobile Engineering, PSG College of Technology, Coimbatore 641004, India.

e-mail: *kpd.auto@psgtech.ac.in*

Jayabalan Arunshankar, DEng. – Department of Instrumentation and Control Systems Engineering, PSG College of Technology, Coimbatore 641004, India.

e-mail: *jas.ice@psgtech.ac.in*

Annex

$$\begin{bmatrix} \dot{C}_{NO} \\ \dot{C}_{NO_2} \\ \dot{\theta}_{NH_3} \\ \dot{C}_{NH_3} \end{bmatrix} = \begin{bmatrix} -r_a C_{O_2} \theta_{NH_3} \emptyset\, V - \frac{1}{2} r_b C_{NO_2} \theta_{NH_3} \emptyset\, V - r_e\, C_{O_2} - \frac{F}{V} + \frac{F}{V} C_{NO,in} \\ -\frac{1}{2} r_b C_{NO} \theta_{NH_3}\, \emptyset\, V + \frac{1}{C_{NO_2}} r_e C_{NO}\, C_{O_2} V\; - \frac{F}{V} + \frac{F}{V} C_{NO_2,in} \\ -\left(r_{d1}\, C_{NH_3} V + r_c\, C_{O_2} V \delta_1 + r_{d2} \delta_2 + r_a C_{NO}\, C_{O_2} V^2 + r_b C_{NO}\, C_{NO_2} V^2\right) + \frac{1}{\theta_{NH_3}} r_{d1}\, C_{NH_3} V \\ -\left[\emptyset\;\, r_{d1}\left(1-\theta_{NH_3}\right) + \frac{F}{V}\right] + \frac{1}{V^*\, C_{NH_3}} r_{d2} \emptyset\, \theta_{NH_3} \delta_2 \end{bmatrix} \begin{bmatrix} C_{NO} \\ C_{NO_2} \\ \theta_{NH_3} \\ C_{NH_3} \end{bmatrix} + \begin{bmatrix} 0 \\ 0 \\ 0 \\ \frac{F}{V} \end{bmatrix} C_{NH_3,in} \tag{10}$$

$$y = \begin{bmatrix} 1 & 0 & 0 & 0 \\ 0 & 1 & 0 & 0 \end{bmatrix} \begin{bmatrix} C_{NO} \\ C_{NO_2} \\ \theta_{NH_3} \\ C_{NH_3} \end{bmatrix} \tag{11}$$